

A FOURTH-ORDER MAXIMUM PRINCIPLE PRESERVING OPERATOR SPLITTING SCHEME FOR THREE-DIMENSIONAL FRACTIONAL ALLEN-CAHN EQUATIONS *

DONGDONG HE[§], KEJIA PAN[†], AND HONGLING HU[‡]

Abstract. In this paper, by using Strang's second-order splitting method, the numerical procedure for the three-dimensional (3D) space fractional Allen-Cahn equation can be divided into three steps. The first and third steps involve an ordinary differential equation, which can be solved analytically. The intermediate step involves a 3D linear fractional diffusion equation, which is solved by the Crank-Nicolson alternating directional implicit (ADI) method. The ADI technique can convert the multidimensional problem into a series of one-dimensional problems, which greatly reduces the computational cost. A fourth-order difference scheme is adopted for discretization of the space fractional derivatives. Finally, Richardson extrapolation is exploited to increase the temporal accuracy. The proposed method is shown to be unconditionally stable by Fourier analysis. Another contribution of this paper is to show that the numerical solutions satisfy the discrete maximum principle under reasonable time step constraint. For fabricated smooth solutions, numerical results show that the proposed method is unconditionally stable and fourth-order accurate in both time and space variables. In addition, the discrete maximum principle is also numerically verified.

Key words. fractional Allen-Cahn equation, operator splitting method, unconditional stability, ADI method, discrete maximum principle

AMS subject classifications. 65M06, 65M12

1. Introduction. In this paper, we investigate the numerical solution of the following space fractional Allen-Cahn equation [1, 4, 15, 29]

$$(1.1) \quad u_t = \varepsilon^2 L_\alpha u - f(u), \quad \mathbf{x} \in \Omega, \quad t \in (0, T],$$

with initial condition

$$(1.2) \quad u(\mathbf{x}, 0) = u_0(x), \quad \mathbf{x} \in \Omega,$$

and the homogeneous Dirichlet boundary condition

$$(1.3) \quad u(\mathbf{x}, t) = 0, \quad \mathbf{x} \text{ on } \partial\Omega, \quad t \in [0, T],$$

where Ω is a rectangular domain, $\Omega = [0, 1]^2$ in two dimension and $\Omega = [0, 1]^3$ in three dimension, $\alpha \in (1, 2]$, and the nonlinear term $f(u)$ is taken as the polynomial double-well potential

$$(1.4) \quad f(u) = u^3 - u.$$

*This research was supported by the Natural Science Foundation of China (Nos. 11402174, 41474103), the President's Fund-Research Start-up Fund from the Chinese University of Hong Kong, Shenzhen, the Excellent Youth Foundation of Hunan Province of China (No. 2018JJ1042) and the Innovation-Driven Project of Central South University (No. 2018CX042).

[§]School of Science and Engineering, The Chinese University of Hong Kong, Shenzhen, Guangdong 518172, China (hedongdong@cuhk.edu.cn)

[†]Corresponding author. School of Mathematics and Statistics, Central South University, Changsha, Hunan 410083, China (pankejia@hotmail.com)

[‡]School of Mathematics and Statistics, Key Laboratory of High Performance Computing and Stochastic Information Processing, Hunan Normal University, Changsha, Hunan 410081, China (honglinghu@hunnu.edu.cn)

Here, the fractional Laplacian operator L_α replaces the standard Laplacian operator. In one dimension, the fractional Laplacian $L_\alpha u$ ($\alpha \in (1, 2)$) for u defined in the interval $x \in [a, b]$ with homogeneous Dirichlet boundary condition is given as follows,

$$(1.5) \quad \mathcal{L}_\alpha u = \mathcal{L}_x^\alpha u := \frac{1}{-2 \cos(\frac{\alpha\pi}{2})} ({}_a D_x^\alpha u + {}_x D_b^\alpha u),$$

where the left and right Riemann-Liouville fractional derivatives are respectively defined as

$${}_a D_x^\alpha u = \frac{1}{\Gamma(2-\alpha)} \frac{d^2}{dx^2} \int_a^x \frac{u(\xi)}{(x-\xi)^{\alpha-1}} d\xi,$$

$${}_x D_b^\alpha u = \frac{1}{\Gamma(2-\alpha)} \frac{d^2}{dx^2} \int_x^b \frac{u(\xi)}{(\xi-x)^{\alpha-1}} d\xi.$$

The fractional operators in two dimension and three dimension can be defined in a similar way, for example, the 3D fractional Laplacian $\mathcal{L}_\alpha u$ is defined as

$$\mathcal{L}_\alpha u = \mathcal{L}_x^\alpha u + \mathcal{L}_y^\alpha u + \mathcal{L}_z^\alpha u.$$

For the case $\alpha = 2$, the above fractional Allen-Cahn equation will be reduced into the standard Allen-Cahn equation, which is widely studied in the literature. When neglecting nonlinear term $f(u)$, equation (1.1) reduces to the fractional diffusion equation, which has been numerically studied extensively in recent years [22, 31, 32, 52].

The fractional Allen-Cahn equation can be viewed as the L^2 -gradient flow of the following fractional analogue Ginzburg-Landau free energy functional

$$(1.6) \quad \mathcal{E}(u) = \int_\Omega F(u) - \frac{1}{2} \varepsilon^2 u L_\alpha u du,$$

with $F(u) = \frac{1}{4}(u^2 - 1)^2$.

The standard Allen-Cahn equation [1] was first introduced to describe the motion of anti-phase boundaries in crystalline solids. It can be considered as the L^2 -gradient flow of the Ginzburg-Landau free energy. Recently, the Allen-Cahn equation, regarded as one of the diffusion-interface phase field models, has been widely applied to many complicated moving interface problems, for example, vesicle membranes, the nucleation of solids and the mixture of two incompressible fluids [9, 10, 11, 23, 45, 47, 48]. It is known that the Allen-Cahn equation has two intrinsic properties: one is the energy decreasing property, the other is the maximum principle [11]. Since the Allen-Cahn equation is a nonlinear partial differential equation, the exact solution is not available. Numerical computations are essentially important to understand the behavior of the solution. In the existing literature, the Allen-Cahn equation was numerically extensively studied [7, 36, 35, 40, 24, 25, 12, 13, 44, 14, 53]. For example, Choi *et al.* [7] proposed an unconditionally gradient stable nonlinear scheme with both discrete maximum principle and energy decreasing properties. And the discrete energy stability can be found in [36, 12, 13, 14, 53]. More recently, the discrete maximum principle is discussed in [20, 35, 40]. However, the implicit-explicit scheme proposed in [40] is only first-order accurate in time variable, the fully discretized Crank-Nicolson scheme proposed in [20] is a nonlinear scheme, and the authors pointed out that it is still remains open to see whether the maximum principle is still true for high-order accurate

linear schemes, which is a difficult issue [40, 20]. Besides, the Allen-Cahn equation was also numerically investigated by using the operator splitting scheme [24, 25, 44].

Recently, fractional differential equations have attracted many attention. For time-fractional diffusion equations, finite difference methods and spectral methods have been used to investigate the solutions [26, 27, 28, 49]. For space fractional differential equations, there are also quite a lot of numerical studies for different equations [46, 42, 43, 21, 41, 17, 2, 3, 54, 20, 37, 51, 34, 30, 8, 34]. In particular, for the above space fractional Allen-Cahn equation (1.1), Bueno-Orovio *et al.* [2] used an implicit finite element method, Burrage *et al.* [3] used a Fourier spectral method, and Hou *et al.* [20] used a finite difference method. One of intrinsic property of the above space fractional Allen-Cahn equation (1.1) is the maximum principle, which says that the value of the solution $u(\mathbf{x}, t)$ is bounded by 1 for any time $t > 0$, provided the initial value $u_0(\mathbf{x})$ is bounded by 1. Although the method of [35, 40] can be extended to the above space fractional Allen-Cahn equation (1.1) with the discrete maximum principle, this method has only a first-order accuracy in time variable. Recently, Hou *et al.* [20] proposed a finite difference scheme with discrete maximum principle, where the method is second-order accurate both in time and space variables. However, due to the nonlinear nature of the scheme and no dimensional splitting techniques, the method of [20] will generally be computationally expensive especially when solving 3D problems. And Song *et al.* [37] first proposed a ADI method for the 2D space fractional Allen-Cahn equation and applied the proposed method to simulate the incompressible two-phase flows by coupling this fractional Allen-Cahn equation and Navier-Stokes equations, an extra linear term is added into the system in order to obtain the unconditional stability. Similar treatments by introducing an extra linear stabilized term for the integer order Allen-Cahn equation can be found in [13, 50, 35, 40]. As far as we aware, there is no study on high-order maximum principle preserving schemes for the space fractional Allen-Cahn equation, which is pointed as an open problem even in the case of the integer order Allen-Cahn equation [40].

In this paper, we will develop a fourth-order maximum principle preserving operator splitting method for solving the 2D and 3D fractional Allen-Cahn equations (1.1). First, by using a second-order operator splitting method, the numerical solution of the fractional Allen-Cahn equation can be obtained by three steps. The first and third steps involve an ordinary differential equation (ODE), which can be solved analytically. The intermediate step involves a 2D/3D fractional diffusion equation, Crank-Nicolson scheme is adopted for time discretization, and the ADI method [33, 39, 18, 6, 19] combined with a fourth-order difference scheme is used for spatial discretization. The ADI technique converts the multidimensional diffusion problem into a series of one-dimensional problems, which greatly reduces the computational cost. Finally, Richardson extrapolation is exploited to increase the temporal accuracy to fourth order. The proposed method does not introduce any extra stabilized term and is shown to be unconditionally stable by the Von Neumann stability analysis for second step and a simple analysis for first and third steps. Another contribution of this paper is to show that the numerical solution satisfies the discrete maximum principle under reasonable time step constraint. Numerical experiments are carried out for both 2D and 3D space fractional Allen-Cahn equations. For fabricated smooth solutions, results confirm that the proposed method is unconditionally stable and fourth-order accurate for both time and space variables. Moreover, the discrete maximum principle is well verified numerically.

The rest of this paper is organized as follows. Section 2 provides the operator

splitting method for the 3D fractional Allen-Cahn equation. Section 3 proves unconditional stability of the proposed method. The discrete maximum principle is obtained in Section 4. Section 5 presents the numerical results which confirm the theoretical results. And the conclusion is given in final section.

2. Numerical method. In the following, we will present the numerical method to solve the 3D fractional Allen-Cahn equation, the proposed method can be straightforwardly applied to solve the 2D fractional Allen-Cahn equation.

For a positive integer N , let $\Delta t = T/N$, $t_n = n\Delta t$. The time domain $[0, T]$ is covered by $\{t_n\}$. Let v^n be the approximation of $v(x, y, z, n\Delta t)$ for an arbitrary function $v(x, y, z, t)$. The solution domain is defined as $\Omega \times [0, T]$ ($\Omega = [0, 1]^3$), which is covered by a uniform grid $\Omega_h = \{(x_i, y_j, z_k, t_n) | x_i = ih_x, y_j = jh_y, z_k = kh_z, t_n = n\Delta t, i = 0, \dots, M_x, j = 0, \dots, M_y, k = 0, \dots, M_z, n = 0, \dots, N\}$, where $h_x = 1/M_x, h_y = 1/M_y, h_z = 1/M_z$. Let $U^n = (U_{i,j,k}^n)_{(M_x+1) \times (M_y+1) \times (M_z+1)}$ be the numerical solution at time level $t = t_n$, the homogeneous Dirichlet boundary condition (1.3) gives

$$U_{0,j,k}^n = U_{M_x,j,k}^n = U_{i,0,k}^n = U_{i,M_y,k}^n = U_{i,j,0}^n = U_{i,j,M_z}^n = 0$$

for any $n = 0, \dots, N$. And we denote

$$\|U^n\|_\infty = \max_{\substack{1 \leq i \leq M_x-1 \\ 1 \leq j \leq M_y-1 \\ 1 \leq k \leq M_z-1}} |U_{i,j,k}^n|.$$

2.1. Temporal discretization. Now we rewrite the fractional Allen-Cahn equation as the following evolution equation,

$$(2.1) \quad \frac{\partial u}{\partial t} = \mathcal{L}_1 u + \mathcal{L}_2 u,$$

where the operators $\mathcal{L}_1, \mathcal{L}_2$ are defined as

$$\mathcal{L}_1 u = -f(u) = u - u^3, \quad \mathcal{L}_2 u = \varepsilon^2 L_\alpha u.$$

According to Strang's second-order splitting method [38], the numerical solution of Eq. (2.1) in the time interval $[t_n, t_{n+1}]$ can be obtained as follows,

$$(2.2) \quad U^{n+1} = \left(\mathcal{L}_1^{\frac{\Delta t}{2}} \circ \mathcal{L}_2^{\Delta t} \circ \mathcal{L}_1^{\frac{\Delta t}{2}} \right) U^n,$$

where $\mathcal{L}_1^{\Delta t}$ and $\mathcal{L}_2^{\Delta t}$ are the evolution operators for $\frac{\partial u}{\partial t} = \mathcal{L}_1 u$ and $\frac{\partial u}{\partial t} = \mathcal{L}_2 u$, respectively.

More precisely, we shall write the above splitting operator into three steps as follows,

$$(2.3) \quad \frac{\partial \tilde{u}}{\partial t} = -\frac{1}{2}f(\tilde{u}) = \frac{1}{2}(\tilde{u} - \tilde{u}^3), \quad \tilde{u}^n = U^n, \quad t \in [t_n, t_{n+1}],$$

$$(2.4) \quad \frac{\partial \bar{u}}{\partial t} = \varepsilon^2 L_\alpha \bar{u} = \varepsilon^2 (\mathcal{L}_x^\alpha \bar{u} + \mathcal{L}_y^\alpha \bar{u} + \mathcal{L}_z^\alpha \bar{u}), \quad \bar{u}^n = \tilde{u}^{n+1}, \quad t \in [t_n, t_{n+1}],$$

$$(2.5) \quad \frac{\partial \hat{u}}{\partial t} = -\frac{1}{2}f(\hat{u}) = \frac{1}{2}(\hat{u} - \hat{u}^3), \quad \hat{u}^n = \bar{u}^{n+1}, \quad t \in [t_n, t_{n+1}].$$

The numerical solution at $t = t_{n+1}$ is given by $U^{n+1} = \hat{u}^{n+1}$.

The first and third steps (2.3) and (2.5) solve the same ODE, which can be calculated analytically [44, 25], i.e.,

$$(2.6) \quad \tilde{u}^{n+1} = \frac{U^n}{\sqrt{(U^n)^2 + (1 - (U^n)^2) e^{-\Delta t}}},$$

$$(2.7) \quad \hat{u}^{n+1} = \frac{\bar{u}^{n+1}}{\sqrt{(\bar{u}^{n+1})^2 + (1 - (\bar{u}^{n+1})^2) e^{-\Delta t}}}.$$

The intermediate step (2.4) involves solving a 3D space fractional diffusion equation. A Crank-Nicolson ADI method is proposed for Eq. (2.4), which will be described in the following.

We first apply the Crank-Nicolson scheme for temporal discretization of Eq. (2.4), i.e.,

$$(2.8) \quad \frac{\bar{u}^{n+1} - \bar{u}^n}{\Delta t} = \varepsilon^2 (\mathcal{L}_x^\alpha + \mathcal{L}_y^\alpha + \mathcal{L}_z^\alpha) \frac{\bar{u}^{n+1} + \bar{u}^n}{2} + O(\Delta t^2),$$

Collecting the terms for \bar{u}^{n+1} and \bar{u}^n in (2.8), one can get

$$(2.9) \quad \left(\frac{1}{\Delta t} - \frac{\varepsilon^2}{2} (\mathcal{L}_x^\alpha + \mathcal{L}_y^\alpha + \mathcal{L}_z^\alpha) \right) \bar{u}^{n+1} = \left(\frac{1}{\Delta t} + \frac{\varepsilon^2}{2} (\mathcal{L}_x^\alpha + \mathcal{L}_y^\alpha + \mathcal{L}_z^\alpha) \right) \bar{u}^n + O(\Delta t^2).$$

Eq. (2.9) is equivalent to

$$(2.10) \quad \begin{aligned} & \frac{1}{\Delta t} \left(1 - \frac{\Delta t \varepsilon^2}{2} \mathcal{L}_x^\alpha \right) \left(1 - \frac{\Delta t \varepsilon^2}{2} \mathcal{L}_y^\alpha \right) \left(1 - \frac{\Delta t \varepsilon^2}{2} \mathcal{L}_z^\alpha \right) \bar{u}^{n+1} \\ &= \frac{1}{\Delta t} \left(1 + \frac{\Delta t \varepsilon^2}{2} \mathcal{L}_x^\alpha \right) \left(1 + \frac{\Delta t \varepsilon^2}{2} \mathcal{L}_y^\alpha \right) \left(1 + \frac{\Delta t \varepsilon^2}{2} \mathcal{L}_z^\alpha \right) \bar{u}^n \\ &+ \frac{\Delta t \varepsilon^4}{4} (\mathcal{L}_x^\alpha \mathcal{L}_y^\alpha + \mathcal{L}_x^\alpha \mathcal{L}_z^\alpha + \mathcal{L}_y^\alpha \mathcal{L}_z^\alpha) (\bar{u}^{n+1} - \bar{u}^n) - \frac{\Delta t^2 \varepsilon^6}{8} \mathcal{L}_y^\alpha \mathcal{L}_x^\alpha \mathcal{L}_z^\alpha (\bar{u}^{n+1} + \bar{u}^n) + O(\Delta t^2). \end{aligned}$$

Since

$$\begin{aligned} & \frac{\Delta t \varepsilon^4}{4} (\mathcal{L}_x^\alpha \mathcal{L}_y^\alpha + \mathcal{L}_x^\alpha \mathcal{L}_z^\alpha + \mathcal{L}_y^\alpha \mathcal{L}_z^\alpha) (\bar{u}^{n+1} - \bar{u}^n) \\ &= \frac{\Delta t \varepsilon^4}{4} (\mathcal{L}_x^\alpha \mathcal{L}_y^\alpha + \mathcal{L}_x^\alpha \mathcal{L}_z^\alpha + \mathcal{L}_y^\alpha \mathcal{L}_z^\alpha) \left(\Delta t \frac{\partial \bar{u}^{n+\frac{1}{2}}}{\partial t} + O(\Delta t)^3 \right) = O(\Delta t^2), \end{aligned}$$

and

$$\frac{\Delta t^2 \varepsilon^8}{8} \mathcal{L}_x^\alpha \mathcal{L}_z^\alpha \mathcal{L}_y^\alpha (\bar{u}^{n+1} + \bar{u}^n) = \frac{\Delta t^2 \varepsilon^8}{8} \mathcal{L}_x^\alpha \mathcal{L}_y^\alpha \mathcal{L}_z^\alpha \left(2\bar{u}^{n+\frac{1}{2}} + O(\Delta t^2) \right) = O(\Delta t^2),$$

Eq. (2.10) is indeed

$$(2.11) \quad \begin{aligned} & \frac{1}{\Delta t} \left(1 - \frac{\Delta t \varepsilon^2}{2} \mathcal{L}_x^\alpha \right) \left(1 - \frac{\Delta t \varepsilon^2}{2} \mathcal{L}_y^\alpha \right) \left(1 - \frac{\Delta t \varepsilon^2}{2} \mathcal{L}_z^\alpha \right) \bar{u}^{n+1} \\ &= \frac{1}{\Delta t} \left(1 + \frac{\Delta t \varepsilon^2}{2} \mathcal{L}_x^\alpha \right) \left(1 + \frac{\Delta t \varepsilon^2}{2} \mathcal{L}_y^\alpha \right) \left(1 + \frac{\Delta t \varepsilon^2}{2} \mathcal{L}_z^\alpha \right) \bar{u}^n + O(\Delta t^2). \end{aligned}$$

The above discretization is only for time.

2.2. Spatial discretization. For spatial discretization, with the homogenous boundary condition (1.3), the second-order difference scheme for the space fractional derivatives is given as [5]

$$(2.12) \quad \mathcal{L}_x^\alpha u \approx -\frac{1}{h_1^\alpha} \sum_{s=i-M_x+1}^{i-1} c_s^\alpha u_{i-s,j,k} = -\frac{1}{h_1^\alpha} \sum_{s=1}^{M_x-1} c_{i-s}^\alpha u_{s,j,k},$$

$$(2.13) \quad \mathcal{L}_y^\alpha u \approx -\frac{1}{h_2^\alpha} \sum_{s=j-M_y+1}^{j-1} c_s^\alpha u_{i,j-s,k} = -\frac{1}{h_2^\alpha} \sum_{s=1}^{M_y-1} c_{j-s}^\alpha u_{i,s,k},$$

$$(2.14) \quad \mathcal{L}_z^\alpha u \approx -\frac{1}{h_3^\alpha} \sum_{s=k-M_z+1}^{k-1} c_s^\alpha u_{i,j,k-s} = -\frac{1}{h_3^\alpha} \sum_{s=1}^{M_z-1} c_{k-s}^\alpha u_{i,j,s},$$

where

$$(2.15) \quad c_0^\alpha = \frac{\Gamma(\alpha+1)}{(\Gamma(\frac{\alpha}{2}+1))^2},$$

$$(2.16) \quad c_s^\alpha = \frac{(-1)^s \Gamma(\alpha+1)}{\Gamma(\frac{\alpha}{2}-s+1)\Gamma(\frac{\alpha}{2}+s+1)} = \left(1 - \frac{\alpha+1}{\frac{\alpha}{2}+s}\right) c_{s-1}^\alpha, \quad \text{for } s \in \mathbb{Z}.$$

Denote the operators $\Delta_x^\alpha, \Delta_y^\alpha, \Delta_z^\alpha$ and the identity operator I as follows,

$$(2.17) \quad [\Delta_x^\alpha u]_{i,j,k} = - \sum_{s=i-M_x+1}^{i-1} c_s^\alpha u_{i-s,j,k} = - \sum_{s=1}^{M_x-1} c_{i-s}^\alpha u_{s,j,k},$$

$$(2.18) \quad [\Delta_y^\alpha u]_{i,j,k} = - \sum_{s=j-M_y+1}^{j-1} c_s^\alpha u_{i,j-s,k} = - \sum_{s=1}^{M_y-1} c_{j-s}^\alpha u_{i,s,k},$$

$$(2.19) \quad [\Delta_z^\alpha u]_{i,j,k} = - \sum_{s=k-M_z+1}^{k-1} c_s^\alpha u_{i,j,k-s} = - \sum_{s=1}^{M_z-1} c_{k-s}^\alpha u_{i,j,s},$$

and

$$(2.20) \quad [Iu]_{i,j,k} = u_{i,j,k}.$$

Let $\mathcal{A}_x^\alpha, \mathcal{A}_y^\alpha, \mathcal{A}_z^\alpha$ be the average operators defined as [16]

$$(2.21) \quad \mathcal{A}_x^\alpha u_{i,j,k} = \frac{\alpha}{24} u_{i-1,j,k} + \left(1 - \frac{\alpha}{12}\right) u_{i,j,k} + \frac{\alpha}{24} u_{i+1,j,k},$$

$$(2.22) \quad \mathcal{A}_y^\alpha u_{i,j,k} = \frac{\alpha}{24} u_{i,j-1,k} + \left(1 - \frac{\alpha}{12}\right) u_{i,j,k} + \frac{\alpha}{24} u_{i,j+1,k},$$

$$(2.23) \quad \mathcal{A}_z^\alpha u_{i,j,k} = \frac{\alpha}{24} u_{i,j,k-1} + \left(1 - \frac{\alpha}{12}\right) u_{i,j,k} + \frac{\alpha}{24} u_{i,j,k+1}.$$

The fourth-order difference scheme for the space fractional derivatives is given as [16, 17]

$$(2.24) \quad (\mathcal{L}_x^\alpha u)_{i,j,k} = \frac{1}{h_1^\alpha} [(\mathcal{A}_x^\alpha)^{-1} \Delta_x^\alpha u]_{i,j,k} + O(h_1^4),$$

$$(2.25) \quad (\mathcal{L}_y^\alpha u)_{i,j,k} = \frac{1}{h_2^\alpha} [(\mathcal{A}_y^\alpha)^{-1} \Delta_y^\alpha u]_{i,j,k} + O(h_2^4),$$

$$(2.26) \quad (\mathcal{L}_z^\alpha u)_{i,j,k} = \frac{1}{h_3^\alpha} [(\mathcal{A}_z^\alpha)^{-1} \Delta_z^\alpha u]_{i,j,k} + O(h_3^4).$$

Substituting (2.24)-(2.26) into (2.11) and evaluating at (x_i, y_j, z_k) , we have

$$\begin{aligned}
 (2.27) \quad & \frac{1}{\Delta t} \left[\left(I - \frac{\Delta t \varepsilon^2}{2h_1^\alpha} (\mathcal{A}_x^\alpha)^{-1} \Delta_x^\alpha \right) \left(I - \frac{\Delta t \varepsilon^2}{2h_2^\alpha} (\mathcal{A}_y^\alpha)^{-1} \Delta_y^\alpha \right) \left(I - \frac{\Delta t \varepsilon^2}{2h_3^\alpha} (\mathcal{A}_z^\alpha)^{-1} \Delta_z^\alpha \right) \bar{u}^{n+1} \right]_{i,j,k} \\
 &= \frac{1}{\Delta t} \left[\left(I + \frac{\Delta t \varepsilon^2}{2h_1^\alpha} (\mathcal{A}_x^\alpha)^{-1} \Delta_x^\alpha \right) \left(I + \frac{\Delta t \varepsilon^2}{2h_2^\alpha} (\mathcal{A}_y^\alpha)^{-1} \Delta_y^\alpha \right) \left(I + \frac{\Delta t \varepsilon^2}{2h_3^\alpha} (\mathcal{A}_z^\alpha)^{-1} \Delta_z^\alpha \right) \bar{u}^n \right]_{i,j,k} \\
 &+ O(\Delta t^2 + h_x^4 + h_y^4 + h_z^4).
 \end{aligned}$$

Neglecting the truncation errors in (2.27), applying the operator $\mathcal{A}_x^\alpha \mathcal{A}_y^\alpha \mathcal{A}_z^\alpha$ to both sides and introducing the intermediate variable u^*, u^{**} , we obtain the D'Yakonov ADI-like scheme [33] as follows,

$$(2.28) \quad [(\mathcal{A}_x^\alpha - \beta_x \Delta_x^\alpha) \bar{u}^*]_{i,j,k} = [(\mathcal{A}_x^\alpha + \beta_x \Delta_x^\alpha)(\mathcal{A}_y^\alpha + \beta_y \Delta_y^\alpha)(\mathcal{A}_z^\alpha + \beta_z \Delta_z^\alpha) \bar{u}^n]_{i,j,k},$$

$$(2.29) \quad [(\mathcal{A}_y^\alpha - \beta_y \Delta_y^\alpha) \bar{u}^{**}]_{i,j,k} = \bar{u}_{i,j,k}^*,$$

$$(2.30) \quad [(\mathcal{A}_z^\alpha - \beta_z \Delta_z^\alpha) \bar{u}^{n+1}]_{i,j,k} = \bar{u}_{i,j,k}^{**},$$

where $\beta_x = \Delta t \varepsilon^2 / (2h_1^\alpha)$, $\beta_y = \Delta t \varepsilon^2 / (2h_2^\alpha)$, $\beta_z = \Delta t \varepsilon^2 / (2h_3^\alpha)$. Each of the above three equations is a one-dimensional linear system and all coefficient matrices are constant matrices whose inverse only need to be computed once during the whole computation. Thus, the above ADI method can be solved very efficiently.

REMARK 2.1. *From the analytical solution (2.7) and homogeneous boundary condition (1.3), one can show that \bar{u}^{n+1} also satisfies the homogeneous boundary condition. Thus, from above ADI scheme, one can see that \bar{u}^{**} satisfies the homogeneous boundary condition in x, y directions and \bar{u}^* satisfies the homogeneous boundary condition in x direction. These conditions are needed in the implementation of the above ADI scheme.*

REMARK 2.2. *The above Crank-Nicolson ADI scheme (2.28)-(2.30) is second-order accurate in time and fourth-order accurate in space. Replacing the average operator \mathcal{A}_x^α , \mathcal{A}_y^α and \mathcal{A}_z^α by the identity operator defined in (2.20), yields the following second-order scheme:*

$$(2.31) \quad [(\mathcal{I} - \beta_x \Delta_x^\alpha) \bar{u}^*]_{i,j,k} = [(\mathcal{I} + \beta_x \Delta_x^\alpha)(\mathcal{I} + \beta_y \Delta_y^\alpha)(\mathcal{I} + \beta_z \Delta_z^\alpha) \bar{u}^n]_{i,j,k},$$

$$(2.32) \quad [(\mathcal{I} - \beta_y \Delta_y^\alpha) \bar{u}^{**}]_{i,j,k} = \bar{u}_{i,j,k}^*,$$

$$(2.33) \quad [(\mathcal{I} - \beta_z \Delta_z^\alpha) \bar{u}^{n+1}]_{i,j,k} = \bar{u}_{i,j,k}^{**}.$$

2.3. Richardson extrapolation. The scheme (2.27) is a higher-order perturbation of the Crank-Nicolson scheme (2.8) in three space variables. Thus, the temporal order of accuracy of the ADI scheme (2.28)-(2.30) is two, which is the same as the Strang's time splitting method (2.3)-(2.5). Consequently, the proposed operator splitting method (2.3)-(2.5) together with the ADI scheme (2.28)-(2.30) will be second-order accurate in time variable and fourth-order accurate in space variable. In order to increase the time accuracy, we apply the following Richardson extrapolation for the final step numerical solution:

$$(2.34) \quad \tilde{U}^N(\Delta t, h_x, h_y, h_z) = \frac{4}{3} U^N(\Delta t, h_x, h_y, h_z) - \frac{1}{3} U^{N/2}(2\Delta t, h_x, h_y, h_z),$$

where $U^N(\Delta t, h_x, h_y, h_z)$, $U^{N/2}(2\Delta t, h_x, h_y, h_z)$ are numerical solutions at the final step by using spatial meshsizes h_x, h_y, h_z and time step $\Delta t, 2\Delta t$, respectively.

If the exact solution has sufficient regularity, then the extrapolated solution \tilde{U}^N is fourth-order accurate in both time and space, see last two columns in Tables 5.1-5.10 for details.

3. Unconditional stability. In this section, we show that the first and third steps in the splitting method (2.3)-(2.5) are unconditionally stable, and then use von Neumann linear stability analysis to prove the unconditional stability of the ADI scheme (2.28)-(2.30) for the second step under the condition that the solution u is periodic and smooth.

LEMMA 3.1. [5] *The coefficients c_s^α have the following properties for $-1 < \alpha \leq 2$*

$$(3.1) \quad \begin{aligned} c_0^\alpha &= \frac{\Gamma(\alpha+1)}{(\Gamma(\frac{\alpha}{2}+1))^2} > 0, \\ c_p^\alpha &= c_{-p}^\alpha \leq 0, \quad \text{for } p = \pm 1, \pm 2, \dots, \\ \sum_{p=-M_{x(y,z)}+1+i, p \neq 0}^{i-1} |c_p^\alpha| &< c_0^\alpha, \quad \text{for } i = 1, \dots, M_{x(y,z)} - 1. \end{aligned}$$

LEMMA 3.2. *Suppose that z is a complex number and $a > 0$ is a real number, then*

$$(3.2) \quad \left| \frac{a-z}{a+z} \right| \leq 1 \quad \text{if and only if } \operatorname{Re}(z) \geq 0.$$

Proof. This lemma is easy to verify. \square

LEMMA 3.3. *At any time level $t = t_n$, for any initial value $U_{i,j,k}^n (i = 0, \dots, M_x, j = 0, \dots, M_y, k = 0, \dots, M_z)$, the numerical solution $u_{i,j,k}^n$ given by (2.6) for the first step in the operator splitting method is unconditionally stable.*

Proof. For a given (i, j, k) ($i = 0, \dots, M_x, j = 0, \dots, M_y, k = 0, \dots, M_z$)

Case 1. if the component $U_{i,j,k}^n$ satisfies $|U_{i,j,k}^n| \leq 1$, then by using (2.6), one has

$$|\tilde{u}_{i,j,k}^{n+1}| = \frac{|U_{i,j,k}^n|}{\sqrt{(U_{i,j,k}^n)^2 + (1 - (U_{i,j,k}^n)^2)e^{-\Delta t}}} \leq \frac{|U_{i,j,k}^n|}{\sqrt{(U_{i,j,k}^n)^2}} = 1.$$

Case 2. if the component $U_{i,j,k}^n$ satisfies $|U_{i,j,k}^n| > 1$, then by using (2.6), one has

$$|\tilde{u}_{i,j,k}^{n+1}| = \frac{|U_{i,j,k}^n|}{\sqrt{(U_{i,j,k}^n)^2(1 - e^{-\Delta t}) + e^{-\Delta t}}} \leq \frac{|U_{i,j,k}^n|}{\sqrt{(1 - e^{-\Delta t}) + e^{-\Delta t}}} = |U_{i,j,k}^n|.$$

Combining these two cases, one has

$$\|\tilde{u}^{n+1}\|_\infty \leq \max \{\|U^n\|_\infty, 1\},$$

which completes the proof of the lemma. \square

LEMMA 3.4. *At any time level $t = t_n$, for any initial value $\hat{u}_{i,j,k}^n (i = 0, \dots, M_x, j = 0, \dots, M_y, k = 0, \dots, M_z)$, the numerical solution $\hat{u}_{i,j,k}^{n+1}$ given by (2.7) for the third step in the operator splitting method is unconditionally stable.*

Proof. The proof of this lemma is similar as Lemma 3.3. \square

LEMMA 3.5. *If u is periodic in x, y and z directions and smooth, then the Crank-Nicolson ADI method (2.28)-(2.30) is unconditionally stable.*

Proof. Let $\bar{u}_{i,j,k}^n$ be the numerical solution of the Crank-Nicolson ADI method (2.28)-(2.30). Since u is periodic and smooth while the first step (2.3) is an ODE, which is solved analytically. Thus, we can assume that the numerical solution $\bar{u}_{i,j,k}^n$ at time level $t = t_n$ is also periodic, which has the following form

$$(3.3) \quad \bar{u}_{i,j,k}^n = \xi^n e^{I(w_x i + w_y j + w_z k)},$$

where ξ^n is the amplitude at time level n , $I = \sqrt{-1}$ is the complex unit, and w_x, w_y and w_z are phase angles in x, y and z directions, respectively.

Substituting (3.3) into (2.28)-(2.30), one can get

$$(3.4) \quad \left| \frac{\bar{u}_{i,j,k}^{n+1}}{\bar{u}_{i,j,k}^n} \right| = \left| \frac{1 + \frac{\alpha(\cos w_x - 1)}{12} - \beta_x \sum_{s=i-M_x+1}^{i-1} c_s^\alpha e^{-I s w_x}}{1 + \frac{\alpha(\cos w_x - 1)}{12} + \beta_x \sum_{s=i-M_x+1}^{i-1} c_s^\alpha e^{-I s w_x}} \right| \cdot \left| \frac{1 + \frac{\alpha(\cos w_y - 1)}{12} - \beta_y \sum_{s=j-M_y+1}^{j-1} c_s^\alpha e^{-I s w_y}}{1 + \frac{\alpha(\cos w_y - 1)}{12} + \beta_y \sum_{s=j-M_y+1}^{j-1} c_s^\alpha e^{-I s w_y}} \right| \cdot \left| \frac{1 + \frac{\alpha(\cos w_z - 1)}{12} - \beta_z \sum_{s=k-M_z+1}^{k-1} c_s^\alpha e^{-I s w_z}}{1 + \frac{\alpha(\cos w_z - 1)}{12} + \beta_z \sum_{s=k-M_z+1}^{k-1} c_s^\alpha e^{-I s w_z}} \right|.$$

From Lemma 3.1, we know that

$$\operatorname{Re} \left(\sum_{s=i-M_x+1}^{i-1} c_s^\alpha e^{-I s w_x} \right) = c_0^\alpha + \sum_{s=i-M_x+1, s \neq 0}^{i-1} c_s^\alpha \cos(s w_x) \geq c_0^\alpha - \sum_{s=i-M_x+1, s \neq 0}^{i-1} |c_s^\alpha| \geq 0.$$

Since $1 < \alpha \leq 2$,

$$1 + \frac{\alpha(\cos w_x - 1)}{12} = \frac{12 + \alpha(\cos w_x - 1)}{12} \geq \frac{12 - 4}{12} > 0.$$

By using Lemma 3.2, one has

$$(3.5) \quad \left| \frac{1 + \frac{\alpha(\cos w_x - 1)}{12} - \beta_x \sum_{s=i-M_x+1}^{i-1} c_s^\alpha e^{-I s w_x}}{1 + \frac{\alpha(\cos w_x - 1)}{12} + \beta_x \sum_{s=i-M_x+1}^{i-1} c_s^\alpha e^{-I s w_x}} \right| \leq 1.$$

Similarly, one has

$$(3.6) \quad \left| \frac{1 + \frac{\alpha(\cos w_y - 1)}{12} - \beta_y \sum_{s=j-M_y+1}^{j-1} c_s^\alpha e^{-I s w_y}}{1 + \frac{\alpha(\cos w_y - 1)}{12} + \beta_y \sum_{s=j-M_y+1}^{j-1} c_s^\alpha e^{-I s w_y}} \right| \leq 1,$$

and

$$(3.7) \quad \left| \frac{1 + \frac{\alpha(\cos w_z - 1)}{12} - \beta_z \sum_{s=k-M_z+1}^{k-1} c_s^\alpha e^{-Is w_z}}{1 + \frac{\alpha(\cos w_z - 1)}{12} + \beta_z \sum_{s=k-M_z+1}^{k-1} c_s^\alpha e^{-Is w_z}} \right| \leq 1.$$

Thus,

$$(3.8) \quad \left| \frac{\bar{u}_{i,j,k}^{n+1}}{\bar{u}_{i,j,k}^n} \right| \leq 1.$$

This completes the proof of the lemma. \square

THEOREM 3.6. *If u is periodic and smooth, then the operator splitting scheme (2.3), (2.28)-(2.30) and (2.5) is unconditionally stable.*

Proof. Combining the results of Lemma 3.3, 3.4, 3.5 gives the theorem. \square

REMARK 3.1. *Since the homogeneous Dirichlet boundary condition (1.3) is used in this paper, the solution can always be extended into a periodic function with a convergent Fourier series expansion if the solution is smooth. Thus, for smooth solutions, the proposed operator splitting method is unconditionally stable.*

4. Discrete maximum principle. **LEMMA 4.1.** *Let matrix \mathbf{C}_x be defined as follows:*

$$(4.1) \quad \mathbf{C}_x = \begin{pmatrix} -c_0^\alpha & 0 & \cdots & \cdots & \cdots & 0 \\ -c_1^\alpha & -c_0^\alpha & -c_{-1}^\alpha & \cdots & \cdots & -c_{-M+1}^\alpha \\ -c_2^\alpha & -c_1^\alpha & -c_0^\alpha & -c_{-1}^\alpha & \cdots & -c_{-M+2}^\alpha \\ \vdots & \vdots & \ddots & \ddots & \ddots & \vdots \\ \vdots & \vdots & \cdots & -c_1^\alpha & -c_0^\alpha & -c_{-1}^\alpha \\ 0 & 0 & \cdots & 0 & 0 & -c_0^\alpha \end{pmatrix}_{(M_x+1) \times (M_x+1)}.$$

Then, \mathbf{C}_x is strictly diagonally dominant [5], i.e.

$$(4.2) \quad |c_{ii}| = c_0^\alpha > \sum_{j \neq i} |c_{ij}|, \quad \text{for } i = 1, \dots, M_x + 1.$$

Similarly, we can define $(M_y + 1) \times (M_y + 1)$ square matrix \mathbf{C}_y and $(M_z + 1) \times (M_z + 1)$ square matrix \mathbf{C}_z , which are also strictly diagonally dominant.

LEMMA 4.2. [35, 40] *Let matrix $\mathbf{B} \in \mathbb{R}^{(M+1) \times (M+1)}$, $\mathbf{A} = a\mathbf{I} - \mathbf{B}$, where $a > 0$, \mathbf{I} is the identity matrix with same size of \mathbf{B} and \mathbf{B} is a negative diagonally dominant matrix, i.e.*

$$\forall i = 1, \dots, M + 1, \quad b_{ii} \leq 0, \quad \text{and} \quad b_{ii} + \sum_{j \neq i} |b_{ij}| \leq 0,$$

then \mathbf{A} is invertible and

$$(4.3) \quad \|\mathbf{A}^{-1}\|_\infty \leq \frac{1}{a}.$$

In the section, we will show that, under certain reasonable time step constraint, the discrete maximum principle for the proposed method is valid.

THEOREM 4.3. *Assume that the initial value $u_0(x)$ satisfies $\max_{x \in \Omega} |u_0(x)| \leq 1$, then the numerical solution $U_{i,j,k}^n$ of (2.3), (2.28)-(2.30) and (2.5) satisfies the discrete maximum principle, i.e., $\|U^n\|_\infty \leq 1$ for any $n = 0, 1, \dots, N$ if the time step satisfies*

$$(4.4) \quad \frac{\alpha + 2}{12} \frac{\max(h_1^\alpha, h_2^\alpha, h_3^\alpha)}{\varepsilon^2 c_0^\alpha} \leq \Delta t \leq \frac{12 - \alpha}{6} \frac{\min(h_1^\alpha, h_2^\alpha, h_3^\alpha)}{\varepsilon^2 c_0^\alpha}.$$

Proof. We prove the theorem by mathematical induction. Obviously, $\|U^n\|_\infty \leq 1$ for $n = 0$ since $U_{i,j,k}^0 = u_0(x_i, y_j, z_k)$. Assume that $\|U^k\|_\infty \leq 1$ ($k \leq n$) is valid, we want to show that $\|U^{n+1}\|_\infty \leq 1$. From (2.6), one can easily obtain that

$$(4.5) \quad \|\tilde{u}^{n+1}\|_\infty \leq 1.$$

Next, we look at the numerical solution \bar{u}^{n+1} of (2.28)-(2.30). Since $\bar{u}^n = \tilde{u}^{n+1}$, one has

$$(4.6) \quad \|\bar{u}^n\|_\infty \leq 1.$$

Let $\bar{u}^n = (\bar{u}_{i,j,k}^n)_{(M_x+1) \times (M_y+1) \times (M_z+1)}$ be a 3D matrix including the boundary points, which are zero values. Denfine matrix \mathbf{D}_x as follows

$$(4.7) \quad \mathbf{D}_x = \begin{pmatrix} -2 & 0 & 0 & \cdots & \cdots & 0 \\ 1 & -2 & 1 & 0 & \cdots & 0 \\ 0 & 1 & -2 & 1 & \ddots & 0 \\ \vdots & \ddots & \ddots & \ddots & \ddots & \vdots \\ 0 & \cdots & 0 & 1 & -2 & 1 \\ 0 & \cdots & 0 & 0 & 0 & -2 \end{pmatrix}_{(M_x+1) \times (M_x+1)}.$$

Another two square matrices \mathbf{D}_y and \mathbf{D}_z can be defined similarly.

From the definition of the operators $\Delta_x^\alpha, \Delta_y^\alpha, \Delta_z^\alpha, I$ in (2.17)-(2.20) and the zero value on boundary points, one can see that the application of operator $\mathcal{A}_z^\alpha + \beta_z \Delta_z^\alpha$ to \bar{u}^n is equivalent to multiply each vector in the third dimension of \bar{u}^n by the matrix $\mathbf{I}_z + \frac{\alpha}{24} \mathbf{D}_z + \beta_z \mathbf{C}_z$ (\mathbf{I}_z is the identity matrix with size $(M_z + 1) \times (M_z + 1)$), the application of operator $\mathcal{A}_y^\alpha + \beta_y \Delta_y^\alpha$ to \bar{u}^n is equivalent to multiply each vector in the second dimension of \bar{u}^n by the matrix $\mathbf{I}_y + \frac{\alpha}{24} \mathbf{D}_y + \beta_y \mathbf{C}_y$ (\mathbf{I}_y is the identity matrix with size $(M_y + 1) \times (M_y + 1)$), and the application of operator $\mathcal{A}_x^\alpha + \beta_x \Delta_x^\alpha$ to \bar{u}^n is equivalent to multiply each vector in the first dimension of \bar{u}^n by the matrix $\mathbf{I}_x + \frac{\alpha}{24} \mathbf{D}_x + \beta_x \mathbf{C}_x$ (\mathbf{I}_x is the identity matrix with size $(M_x + 1) \times (M_x + 1)$).

In addition, (2.28)-(2.30) is equivalent to

$$(4.8) \quad [(\mathcal{A}_x^\alpha - \beta_x \Delta_x^\alpha)(\mathcal{A}_y^\alpha - \beta_y \Delta_y^\alpha)(\mathcal{A}_z^\alpha - \beta_z \Delta_z^\alpha) \bar{u}^{n+1}]_{i,j,k} = [(\mathcal{A}_x^\alpha + \beta_x \Delta_x^\alpha)(\mathcal{A}_y^\alpha + \beta_y \Delta_y^\alpha)(\mathcal{A}_z^\alpha + \beta_z \Delta_z^\alpha) \bar{u}^n]_{i,j,k},$$

which further yields

$$(4.9) \quad \bar{u}_{i,j,k}^{n+1} = \left[(\mathcal{A}_z^\alpha - \beta_z \Delta_z^\alpha)^{-1} (\mathcal{A}_y^\alpha - \beta_y \Delta_y^\alpha)^{-1} (\mathcal{A}_x^\alpha - \beta_x \Delta_x^\alpha)^{-1} (\mathcal{A}_x^\alpha + \beta_x \Delta_x^\alpha) (\mathcal{A}_y^\alpha + \beta_y \Delta_y^\alpha) (\mathcal{A}_z^\alpha + \beta_z \Delta_z^\alpha) \bar{u}^n \right]_{i,j,k},$$

where the application of operator $(\mathcal{A}_z^\alpha - \beta_z \Delta_z^\alpha)^{-1}$ to a 3D matrix is equivalent to multiply each vector in the third dimension of this 3D matrix by the matrix $(\mathbf{I}_z + \frac{\alpha}{24} \mathbf{D}_z - \beta_z \mathbf{C}_z)^{-1}$, the application of operator $(\mathcal{A}_y^\alpha - \beta_y \Delta_y^\alpha)^{-1}$ to a 3D matrix is equivalent to multiply each vector in the second dimension of this 3D matrix by the matrix $(\mathbf{I}_y + \frac{\alpha}{24} \mathbf{D}_y - \beta_y \mathbf{C}_y)^{-1}$, and the application of operator $(\mathcal{A}_x^\alpha - \beta_x \Delta_x^\alpha)^{-1}$ to a 3D matrix is equivalent to multiply each vector in the first dimension of this 3D matrix by the matrix $(\mathbf{I}_x + \frac{\alpha}{24} \mathbf{D}_x - \beta_x \mathbf{C}_x)^{-1}$.

Therefore, it is easy to check that $\bar{u}^{n+1} = (\bar{u}_{i,j,k}^{n+1})_{(M_x+1) \times (M_y+1) \times (M_z+1)}$ can be obtained from $\bar{u}^n = (\bar{u}_{i,j,k}^n)_{(M_x+1) \times (M_y+1) \times (M_z+1)}$ through a series of one-dimensional vector transformations as follows:

- (i) Multiplying each vector in the third dimension of \bar{u}^n by the matrix $\mathbf{I}_z + \frac{\alpha}{24} \mathbf{D}_z + \beta_z \mathbf{C}_z$,
- (ii) Multiplying each vector in the second dimension of resulting matrix in (i) by the matrix $\mathbf{I}_y + \frac{\alpha}{24} \mathbf{D}_y + \beta_y \mathbf{C}_y$,
- (iii) Multiplying each vector in the first dimension of resulting matrix in (ii) by the matrix $\mathbf{I}_x + \frac{\alpha}{24} \mathbf{D}_x + \beta_x \mathbf{C}_x$,
- (iv) Multiplying each vector in the first dimension of resulting matrix in (iii) by the matrix $(\mathbf{I}_x + \frac{\alpha}{24} \mathbf{D}_x - \beta_x \mathbf{C}_x)^{-1}$,
- (v) Multiplying each vector in the second dimension of resulting matrix in (iv) by the matrix $(\mathbf{I}_y + \frac{\alpha}{24} \mathbf{D}_y - \beta_y \mathbf{C}_y)^{-1}$,
- (vi) Multiplying each vector in the third dimension of resulting matrix in (v) by the matrix $(\mathbf{I}_z + \frac{\alpha}{24} \mathbf{D}_z - \beta_z \mathbf{C}_z)^{-1}$.

If condition (4.4) is satisfied, then

$$(4.10) \quad 1 - \frac{\alpha}{12} - \beta_z c_0^\alpha > 0,$$

and

$$(4.11) \quad \sum_j \left| \delta_{i,j} + \frac{\alpha}{24} d_{i,j} + \beta_z c_{i,j} \right| = 1 - \frac{\alpha}{12} - \beta_z c_0^\alpha < 1, \quad \text{for } i = 1, M_z + 1,$$

$$(4.12) \quad \begin{aligned} \sum_j \left| \delta_{i,j} + \frac{\alpha}{24} d_{i,j} + \beta_z c_{i,j} \right| &\leq 1 - \frac{\alpha}{12} - \beta_z c_0^\alpha + \frac{\alpha}{24} + \frac{\alpha}{24} + \beta_z \sum_{j \neq i} |c_{i,j}| \\ &= 1 - \beta_z \left(c_0^\alpha - \sum_{j \neq i} |c_{i,j}| \right) \\ &< 1, \quad \text{for } i = 2, \dots, M_z. \end{aligned}$$

Thus,

$$(4.13) \quad \left\| \mathbf{I}_z + \frac{\alpha}{24} \mathbf{D}_z + \beta_z \mathbf{C}_z \right\|_\infty < 1.$$

By using (4.6) and (4.13), one gets

$$(4.14) \quad \|(\mathcal{A}_z^\alpha + \beta_z \Delta_z^\alpha) \bar{u}^n\|_\infty \leq \left\| \mathbf{I}_z + \frac{\alpha}{24} \mathbf{D}_z + \beta_z \mathbf{C}_z \right\|_\infty \cdot \|\bar{u}^n\|_\infty \leq 1.$$

Similarly,

$$(4.15) \quad \left\| \mathbf{I}_y + \frac{\alpha}{24} \mathbf{D}_y + \beta_y \mathbf{C}_y \right\|_\infty < 1, \quad \left\| \mathbf{I}_x + \frac{\alpha}{24} \mathbf{D}_x + \beta_x \mathbf{C}_x \right\|_\infty < 1.$$

Therefore,

$$(4.16) \quad \|(\mathcal{A}_y^\alpha + \beta_y \Delta_y^\alpha)(\mathcal{A}_z^\alpha + \beta_z \Delta_z^\alpha) \bar{u}^n\|_\infty \leq 1,$$

and

$$(4.17) \quad \|(\mathcal{A}_x^\alpha + \beta_x \Delta_x^\alpha)(\mathcal{A}_y^\alpha + \beta_y \Delta_y^\alpha)(\mathcal{A}_z^\alpha + \beta_z \Delta_z^\alpha) \bar{u}^n\|_\infty \leq 1.$$

If condition (4.4) is satisfied, then

$$(4.18) \quad \frac{\alpha}{12} - \beta_x c_0^\alpha = \frac{\alpha}{12} - \frac{\Delta t \varepsilon^2}{2h_1^\alpha} c_0^\alpha \leq 0,$$

$$(4.19) \quad -\frac{\alpha}{24} - \beta_x c_1^\alpha = -\frac{\alpha}{24} - \frac{\Delta t \varepsilon^2}{2h_1^\alpha} (1 - \frac{\alpha+1}{\frac{\alpha}{2}+1}) c_0^\alpha = -\frac{\alpha}{24} + \frac{\Delta t \varepsilon^2}{2h_1^\alpha} \frac{\alpha}{\alpha+2} c_0^\alpha \geq 0,$$

where Eq.(2.16) is used.

Now for matrix $-\frac{\alpha}{24}\mathbf{D}_x + \beta_x \mathbf{C}_x$, one has

$$(4.20) \quad \sum_{j \neq i} \left| -\frac{\alpha}{24} d_{i,j} + \beta_x c_{i,j} \right| = 0 \leq -\frac{\alpha}{12} + \beta_x c_0^\alpha = -\left(-\frac{\alpha}{24} d_{i,i} + \beta_x c_{i,i} \right), \quad \text{for } i = 1, M_x + 1,$$

and

$$\begin{aligned} \sum_{j \neq i} \left| -\frac{\alpha}{24} d_{i,j} + \beta_x c_{i,j} \right| &= \sum_{j \neq i, i \pm 1} \left| -\frac{\alpha}{24} d_{i,j} + \beta_x c_{i,j} \right| + \left(-\frac{\alpha}{24} - \beta_x c_1^\alpha \right) + \left(-\frac{\alpha}{24} - \beta_x c_{-1}^\alpha \right), \\ &= -\frac{\alpha}{12} + \sum_{j \neq i, i \pm 1} \beta_x |c_{i,j}| + (-\beta_x c_1^\alpha) + (-\beta_x c_{-1}^\alpha) \\ &= -\frac{\alpha}{12} + \sum_{j \neq i} \beta_x |c_{i,j}| \\ &\leq -\frac{\alpha}{12} + \beta_x |c_{i,i}| \\ &= -\frac{\alpha}{12} + \beta_x c_0^\alpha \\ (4.21) \quad &= -\left(-\frac{\alpha}{24} d_{i,i} + \beta_x c_{i,i} \right), \quad \text{for } i = 2, \dots, M_x. \end{aligned}$$

Thus, $-\frac{\alpha}{24}\mathbf{D}_x + \beta_x \mathbf{C}_x$ is a negative diagonally dominant matrix. By using Lemma 4.2, one has

$$(4.22) \quad \left\| \left(\mathbf{I}_x + \frac{\alpha}{24} \mathbf{D}_x - \beta_x \mathbf{C}_x \right)^{-1} \right\|_\infty \leq 1.$$

Applying the above condition and using (4.17), one has

$$(4.23) \quad \left\| (\mathcal{A}_x^\alpha - \beta_x \Delta_x^\alpha)^{-1} (\mathcal{A}_x^\alpha + \beta_x \Delta_x^\alpha) (\mathcal{A}_y^\alpha + \beta_y \Delta_y^\alpha) (\mathcal{A}_z^\alpha + \beta_z \Delta_z^\alpha) \bar{u}^n \right\|_\infty \leq 1,$$

Similarly, if condition (4.4) is satisfied, one has

$$(4.24) \quad \left\| \left(\mathbf{I}_y + \frac{\alpha}{24} \mathbf{D}_y - \beta_y \mathbf{C}_y \right)^{-1} \right\|_\infty \leq 1, \quad \left\| \left(\mathbf{I}_z + \frac{\alpha}{24} \mathbf{D}_z - \beta_z \mathbf{C}_z \right)^{-1} \right\|_\infty \leq 1.$$

Thus,

$$(4.25) \quad \left\| (\mathcal{A}_y^\alpha - \beta_y \Delta_y^\alpha)^{-1} (\mathcal{A}_x^\alpha - \beta_x \Delta_x^\alpha)^{-1} (\mathcal{A}_x^\alpha + \beta_x \Delta_x^\alpha) (\mathcal{A}_y^\alpha + \beta_y \Delta_y^\alpha) (\mathcal{A}_z^\alpha + \beta_z \Delta_z^\alpha) \bar{u}^n \right\|_\infty \leq 1,$$

and

$$(4.26) \quad \left\| (\mathcal{A}_z^\alpha - \beta_z \Delta_z^\alpha)^{-1} (\mathcal{A}_y^\alpha - \beta_y \Delta_y^\alpha)^{-1} (\mathcal{A}_x^\alpha - \beta_x \Delta_x^\alpha)^{-1} (\mathcal{A}_x^\alpha + \beta_x \Delta_x^\alpha) (\mathcal{A}_y^\alpha + \beta_y \Delta_y^\alpha) (\mathcal{A}_z^\alpha + \beta_z \Delta_z^\alpha) \bar{u}^n \right\|_\infty \leq 1.$$

This yields

$$(4.27) \quad \|\bar{u}^{n+1}\|_\infty \leq 1.$$

From (2.7), one can obtain that

$$(4.28) \quad \|\hat{u}^{n+1}\|_\infty \leq 1.$$

Thus,

$$(4.29) \quad \|U^{n+1}\|_\infty = \|\hat{u}^{n+1}\|_\infty \leq 1.$$

This completes the proof of the theorem. \square

REMARK 4.1. *The first entry in the first row and the last entry in the last row in both matrices $\mathbf{C}_{x(y,z)}$ and $\mathbf{D}_{x(y,z)}$ can take arbitrary numbers due to homogeneous Dirichlet boundary conditions. Here we set these two elements the same as the diagonal entry of matrices $\mathbf{C}_{x(y,z)}$ and $\mathbf{D}_{x(y,z)}$ so that Lemma 4.2 can be directly applied when obtaining the estimate (4.22).*

The theoretical results in previous sections also hold for the second-order scheme (2.3), (2.31)-(2.33) and (2.5) with some minor changes. For example, Theorem 4.3 will become

THEOREM 4.4. *Assume that the initial value $u_0(x)$ satisfies $\max_{x \in \Omega} |u_0(x)| \leq 1$, then the numerical solution $U_{i,j,k}^n$ of (2.3), (2.31)-(2.33) and (2.5) satisfies the discrete maximum principle, i.e., $\|U^n\|_\infty \leq 1$ for any $n = 0, 1, \dots, N$ if the time step satisfies*

$$(4.30) \quad \Delta t \leq 2 \frac{\min(h_1^\alpha, h_2^\alpha, h_3^\alpha)}{\varepsilon^2 c_0^\alpha}.$$

Proof. To prove the above theorem, the main difference is that the matrices \mathbf{D}_x , \mathbf{D}_y and \mathbf{D}_z should be changed into a zero matrix. Other parts of the proof are basically the same as Theorem 4.3. \square

5. Numerical results. Our code is written in Matlab and the programs are carried out on a desktop with Intel CPU i7-4790K (4.00GHz) and 16GB RAM.

5.1. Convergence and stability study. In order to numerically test the accuracy of the numerical method, we use exact solutions with sufficient regularity in this subsection as the testing examples.

EXAMPLE 5.1. *In this example, we consider the 2D space fractional Allen-Cahn equation with the exact solution*

$$(5.1) \quad u(x, y, t) = e^{-t} x^4 (1-x)^4 y^4 (1-y)^4,$$

TABLE 5.1
 L^∞ -norm errors and CPU times (in seconds) for Example 5.1 with $\alpha = 1.2$.

Δt	h	CPU	$\ U^N - u^N\ _\infty$	order ₁	$\ \tilde{U}^N - u^N\ _\infty$	order ₂
1/16	1/16	0.02s	1.79E-08		5.45E-10	
1/32	1/32	0.07s	4.37E-09	2.03	3.41E-11	4.00
1/64	1/64	0.23s	1.09E-09	2.01	4.19E-12	3.02
1/128	1/128	0.98s	2.71E-10	2.00	3.27E-13	3.68
1/256	1/256	7.44s	6.78E-11	2.00	2.50E-14	3.71

TABLE 5.2
 L^∞ -norm errors and CPU times (in seconds) for Example 5.1 with $\alpha = 1.5$.

Δt	h	CPU	$\ U^N - u^N\ _\infty$	order ₁	$\ \tilde{U}^N - u^N\ _\infty$	order ₂
1/16	1/16	0.02s	1.48E-08		1.04E-09	
1/32	1/32	0.07s	3.51E-09	2.08	6.48E-11	4.00
1/64	1/64	0.23s	8.66E-10	2.02	4.06E-12	4.00
1/128	1/128	0.97s	2.16E-10	2.00	2.54E-13	4.00
1/256	1/256	7.43s	5.39E-11	2.00	1.72E-14	3.88

so that the exact solution has a sufficient regularity. And in this example, the equation needs to be modified with a source term

$$\begin{aligned}
f(x, y, t) = & \frac{\varepsilon^2}{2 \cos(\frac{\alpha\pi}{2})} e^{-t} \left[\frac{\Gamma(5)}{\Gamma(5-\alpha)} (x^{4-\alpha} + (1-x)^{4-\alpha}) - \frac{4\Gamma(6)}{\Gamma(6-\alpha)} (x^{5-\alpha} + (1-x)^{5-\alpha}) \right. \\
& + \frac{6\Gamma(7)}{\Gamma(7-\alpha)} (x^{6-\alpha} + (1-x)^{6-\alpha}) - \frac{4\Gamma(8)}{\Gamma(8-\alpha)} (x^{7-\alpha} + (1-x)^{7-\alpha}) + \frac{\Gamma(9)}{\Gamma(9-\alpha)} (x^{8-\alpha} + (1-x)^{8-\alpha}) \left. \right] y^4 (1-y)^4 \\
& + \frac{\varepsilon^2}{2 \cos(\frac{\alpha\pi}{2})} e^{-t} \left[\frac{\Gamma(5)}{\Gamma(5-\alpha)} (y^{4-\alpha} + (1-y)^{4-\alpha}) - \frac{4\Gamma(6)}{\Gamma(6-\alpha)} (y^{5-\alpha} + (1-y)^{5-\alpha}) \right. \\
& + \frac{6\Gamma(7)}{\Gamma(7-\alpha)} (y^{6-\alpha} + (1-y)^{6-\alpha}) - \frac{4\Gamma(8)}{\Gamma(8-\alpha)} (y^{7-\alpha} + (1-y)^{7-\alpha}) + \frac{\Gamma(9)}{\Gamma(9-\alpha)} (y^{8-\alpha} + (1-y)^{8-\alpha}) \left. \right] x^4 (1-x)^4 \\
& + e^{-3t} x^{12} (1-x)^{12} y^{12} (1-y)^{12} - 2e^{-t} x^4 (1-x)^4 y^4 (1-y)^4.
\end{aligned}$$

The initial condition is given according to this exact solution and ε is set to be 0.1.

We carry out numerical accuracy test for $1 < \alpha \leq 2$. We measure the numerical errors $e_1(\Delta t, h_x, h_y, h_z) = u - U(\Delta t, h_x, h_y, h_z)$ and $e_2(\Delta t, h_x, h_y, h_z) = u - \tilde{U}(\Delta t, h_x, h_y, h_z)$ at time $T = 1$ in the L^∞ -norm, and compute the convergence orders according to

$$\text{order}_1 = \log_2 \left(\frac{\|e_1(\Delta t, h_x, h_y, h_z)\|_\infty}{\|e_1(\Delta t/2, h_x/2, h_y/2, h_z/2)\|_\infty} \right),$$

and

$$\text{order}_2 = \log_2 \left(\frac{\|e_2(\Delta t, h_x, h_y, h_z)\|_\infty}{\|e_2(\Delta t/2, h_x/2, h_y/2, h_z/2)\|_\infty} \right).$$

Table 5.1-Table 5.4 list the errors and the corresponding convergence orders for $\alpha = 1.2, 1.5, 1.8, 2$ in the L^∞ -norm using the same spatial meshsize $h = h_x = h_y = h_z$ while Table 5.5 lists the errors and the corresponding convergence orders for $\alpha = 1.5$

TABLE 5.3
 L^∞ -norm errors and CPU times (in seconds) for Example 5.1 with $\alpha = 1.8$.

Δt	h	CPU	$\ U^N - u^N\ _\infty$	order ₁	$\ \tilde{U}^N - u^N\ _\infty$	order ₂
1/16	1/16	0.02s	1.08E-08		1.96E-09	
1/32	1/32	0.06s	2.37E-09	2.19	1.17E-10	4.06
1/64	1/64	0.23s	5.71E-10	2.05	7.03E-12	4.06
1/128	1/128	0.97s	1.41E-10	2.01	4.30E-13	4.03
1/256	1/256	7.43s	3.53E-11	2.00	2.69E-14	4.00

TABLE 5.4
 L^∞ -norm errors and CPU times (in seconds) for Example 5.1 with $\alpha = 2.0$.

Δt	h	CPU	$\ U^N - u^N\ _\infty$	order ₁	$\ \tilde{U}^N - u^N\ _\infty$	order ₂
1/16	1/16	0.02s	7.94E-09		2.88E-09	
1/32	1/32	0.06s	1.56E-09	2.34	1.80E-10	3.99
1/64	1/64	0.23s	3.78E-10	2.05	1.13E-11	4.00
1/128	1/128	0.97s	9.39E-11	2.01	7.06E-13	4.00
1/256	1/256	7.43s	2.35E-11	2.00	4.42E-14	4.00

TABLE 5.5
 L^∞ -norm errors and CPU times (in seconds) for Example 5.1 with $\alpha = 1.5$ using unequal meshsizes in x and y directions.

Δt	h_x	h_y	CPU	$\ U^N - u^N\ _\infty$	order ₁	$\ \tilde{U}^N - u^N\ _\infty$	order ₂
1/16	1/16	1/32	0.03s	1.43E-08		9.83E-09	
1/32	1/32	1/64	0.10s	3.48E-09	2.04	5.89E-11	4.06
1/64	1/64	1/128	0.29s	8.64E-10	2.01	3.63E-12	4.02
1/128	1/128	1/256	1.94s	2.16E-10	2.00	2.22E-13	4.03
1/256	1/256	1/512	17.0s	5.39E-11	2.00	1.72E-14	3.69

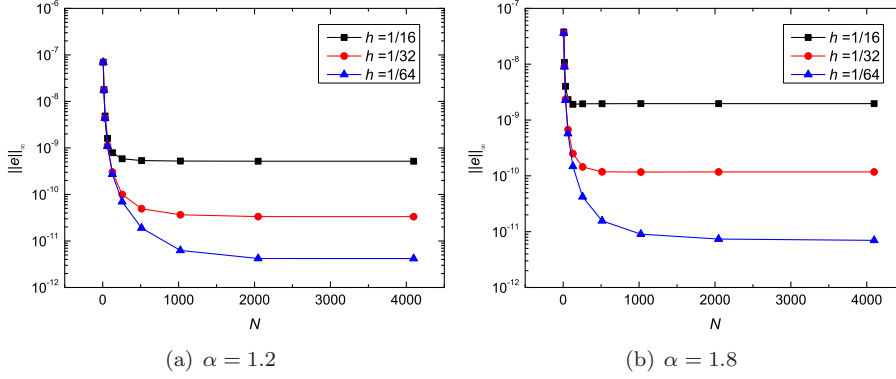
in the L^∞ -norm using different spatial meshsizes. As we can see that these results confirm second-order accuracy in time variable and fourth-order accuracy in space variable if the Richardson extrapolation (2.34) is not applied. But the results is fourth-order accurate both in time and space variables if the Richardson extrapolation (2.34) is applied. Additionally, the computational time in seconds is also provided in Table 5.1-Table 5.5, as we can see that the computational time for $\Delta t = h = \frac{1}{256}$ is less than 10 seconds, and the computational time for $\Delta t = h_x = \frac{1}{256}, h_y = \frac{1}{512}$ is less than 20 seconds. And the method is extremely accurate, the error between the extrapolated solution and exact solution is in the order of 10^{-14} when $\Delta t = h = \frac{1}{256}$ and $\Delta t = h_x = \frac{1}{256}, h_y = \frac{1}{512}$, which is nearly the machine accuracy.

To show the unconditional stability, we fix h and vary Δt , results for $\alpha = 1.2$ and $\alpha = 1.8$ are plotted in Figure 5.1. As one can see that these results clearly show that the time step is not related to the spatial meshsize, and as the spatial meshsize goes to zero, the dominant error comes from the temporal part.

EXAMPLE 5.2. In this example, we consider the 3D space fractional Allen-Cahn equation with the exact solution

$$(5.2) \quad u(x, y, t) = e^{-t} x^4 (1-x)^4 y^4 (1-y)^4 z^4 (1-z)^4.$$

The source term and initial condition are given according to this exact solution, in

FIG. 5.1. Numerical results for Example 5.1 with fixed h but varying Δt .TABLE 5.6
 L^∞ -norm errors and CPU times (in seconds) for Example 5.2 with $\alpha = 1.2$.

Δt	h	CPU	$\ U^N - u^N\ _\infty$	order ₁	$\ \tilde{U}^N - u^N\ _\infty$	order ₂
1/8	1/8	0.01s	2.79E-10		4.82E-11	
1/16	1/16	0.07s	6.10E-11	2.19	2.99E-12	4.01
1/32	1/32	0.42s	1.47E-11	2.05	1.87E-13	4.00
1/64	1/64	6.28s	3.65E-12	2.01	1.58E-14	3.56
1/128	1/128	110s	9.09E-13	2.00	1.24E-15	3.68

addition, ε is set to be 0.1.

Again, we carry out numerical accuracy test for $1 < \alpha \leq 2$. Table 5.6-Table 5.9 list the errors and the corresponding convergence orders for $\alpha = 1.2, 1.5, 1.8, 2$ in the L^∞ -norm using the same spatial meshsize $h = h_x = h_y = h_z$ while Table 5.5 lists the errors and the corresponding convergence orders for $\alpha = 1.5$ in the L^∞ -norm using different spatial meshsizes. As we can see that these results confirm second-order accuracy in time variable and fourth-order accuracy in space variable if the Richardson extrapolation (2.34) is not applied. But the results is fourth-order accurate both in time and space variables if the Richardson extrapolation (2.34) is applied. Additionally, the computational time in seconds is also provided in Table 5.6-Table 5.10, as we can see that the computational time for $\Delta t = h = \frac{1}{128}$ is less than 120 seconds and the computational time for $\Delta t = h_x = \frac{1}{128}, h_y = \frac{1}{160}, h_z = \frac{1}{256}$ is less than 300 seconds. And the method is extremely accurate, the error between the extrapolated solution and exact solution is in the order of 10^{-15} when $\Delta t = h = \frac{1}{128}$ and in the order of 10^{-16} when $\Delta t = h_x = \frac{1}{128}, h_y = \frac{1}{160}, h_z = \frac{1}{256}$, which are both nearly the machine accuracy.

To show the unconditional stability, we fix h and vary Δt , results for $\alpha = 1.2$ and $\alpha = 1.8$ are plotted in Figure 5.2. As one can see that these results clearly show that the time step is not related to the spatial meshsize, and as the spatial meshsize goes to zero, the dominant error comes from the temporal part.

5.2. Numerical tests for discrete maximum principle. EXAMPLE 5.3. *In this example, we consider the 2D space fractional Allen-Cahn equation with initial*

TABLE 5.7
 L^∞ -norm errors and CPU times (in seconds) for Example 5.2 with $\alpha = 1.5$.

Δt	h	CPU	$\ U^N - u^N\ _\infty$	order ₁	$\ \tilde{U}^N - u^N\ _\infty$	order ₂
1/8	1/8	0.01s	2.53E-10		9.13E-11	
1/16	1/16	0.07s	4.61E-11	2.46	5.61E-12	4.02
1/32	1/32	0.42s	1.05E-11	2.14	3.50E-13	4.00
1/64	1/64	6.27s	2.56E-12	2.04	2.19E-14	4.00
1/128	1/128	110s	6.35E-13	2.01	1.37E-15	4.00

TABLE 5.8
 L^∞ -norm errors and CPU times (in seconds) for Example 5.2 with $\alpha = 1.8$.

Δt	h	CPU	$\ U^N - u^N\ _\infty$	order ₁	$\ \tilde{U}^N - u^N\ _\infty$	order ₂
1/8	1/8	0.01s	2.31E-10		1.51E-10	
1/16	1/16	0.07s	2.90E-11	2.99	9.19E-12	4.04
1/32	1/32	0.42s	5.53E-12	2.39	5.71E-13	4.01
1/64	1/64	6.26s	1.28E-12	2.12	3.57E-14	4.00
1/128	1/128	110s	3.12E-13	2.03	2.23E-15	4.00

TABLE 5.9
 L^∞ -norm errors and CPU times (in seconds) for Example 5.2 with $\alpha = 2.0$.

Δt	h	CPU	$\ U^N - u^N\ _\infty$	order ₁	$\ \tilde{U}^N - u^N\ _\infty$	order ₂
1/8	1/8	0.01s	2.22E-10		1.91E-10	
1/16	1/16	0.06s	1.92E-11	3.53	1.15E-11	4.05
1/32	1/32	0.42s	2.93E-12	2.71	7.13E-13	4.01
1/64	1/64	6.23s	7.17E-13	2.03	4.44E-14	4.00
1/128	1/128	109s	1.79E-13	2.00	2.78E-15	4.00

TABLE 5.10
 L^∞ -norm errors and CPU times (in seconds) for Example 5.2 with $\alpha = 1.5$ using unequal meshsizes in x , y and z directions.

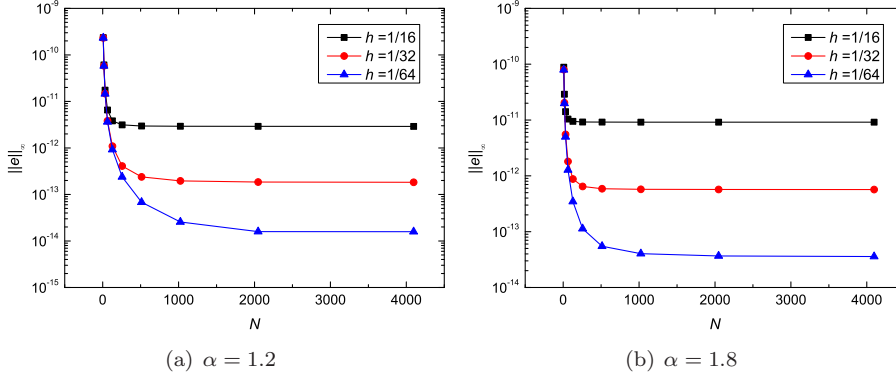
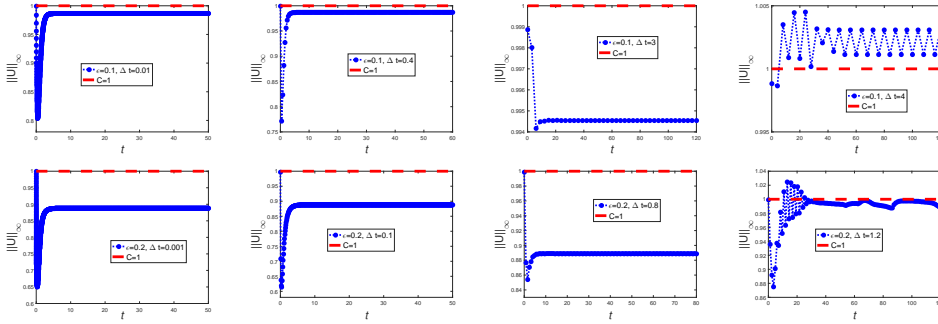
Δt	h_x	h_y	h_z	CPU	$\ U^N - u^N\ _\infty$	order ₁	$\ \tilde{U}^N - u^N\ _\infty$	order ₂
1/8	1/8	1/10	1/16	0.02s	2.06E-10		5.94E-11	
1/16	1/16	1/20	1/32	0.10s	4.33E-11	2.25	3.53E-12	4.07
1/32	1/32	1/40	1/64	0.96s	1.03E-11	2.07	2.11E-13	4.06
1/64	1/64	1/80	1/128	17.2s	2.54E-12	2.02	1.30E-14	4.03
1/128	1/128	1/160	1/256	280.s	6.34E-13	2.00	8.29E-16	3.97

condition

$$(5.3) \quad u_0(x, y) = 0.95 \times \text{rand}(x, y) + 0.05,$$

where zero boundary values are set for the initial condition $u_0(x, y)$. Moreover, α is set to be 1.7.

For this example, we fix $h = 0.05$ but vary ε and Δt . For $\varepsilon = 0.1$, the maximum principle condition (4.4) requires $0.1508 \leq \Delta t \leq 0.4358$. The top four sub-figures in Figure 5.3 show that the maximum values of the numerical solutions are bounded by 1 if $\Delta t = 0.01$, $\Delta t = 0.4$, and $\Delta t = 3$ but exceed 1 if $\Delta t = 4$. For $\varepsilon = 0.2$, the maximum principle condition (4.4) requires $0.0377 \leq \Delta t \leq 0.1089$. The lower four

FIG. 5.2. Numerical results for Example 5.2 with fixed h but varying Δt .FIG. 5.3. Numerical results with $\alpha = 1.6$ and $h = 0.05$: the maximum values of solution with different Δt and ε .

sub-figures in Figure 5.3 show the maximum values of the numerical solutions are bounded by 1 if $\Delta t = 0.001$, $\Delta t = 0.1$, and $\Delta t = 0.4$ but exceed 1 if $\Delta t = 1.2$. These numerical results suggest that the constraint (4.4) for time step size to achieve the discrete maximum principle is only a sufficient condition. In practice, the maximum principle is still valid if a time step size with much smaller values or larger values is adopted.

EXAMPLE 5.4. In this example, we consider the 2D space fractional Allen-Cahn equation with initial condition

$$(5.4) \quad u_0(x, y) = 0.1 \times \text{rand}(x, y) - 0.05,$$

where zero boundary values are set for the initial condition $u_0(x, y)$.

In this example, we first fix $h = 0.01$, $\alpha = 1.7$ and $\varepsilon = 0.02$ but vary Δt . The maximum principle condition (4.4) requires $0.1776 \leq \Delta t \leq 0.4945$. Figure 5.4 shows the maximum values of the numerical solutions are bounded by 1 when $\Delta t = 0.01$ and $\Delta t = 0.4$. However, the maximum value exceeds 1 when Δt increases to 2.

Now we investigate the effects of fractional diffusion on phase separation and coarsening process. We set $h = 0.01$, $\varepsilon = 0.02$, $\Delta t = 0.5$ and $\alpha = 1.2, 1.5, 1.8$. Starting from random initial values, the snapshots of the contours for the numerical solutions at $t = 5, 20, 40, 80$ are shown in Figure 5.5. We see that reducing the fractional order yields to a thinner interfaces that allows smaller bulk regions and a much more

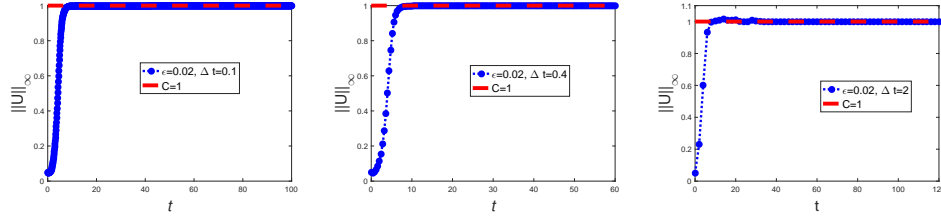


FIG. 5.4. Numerical results with $\alpha = 1.7, \varepsilon = 0.02, h = 0.01$: the maximum values of solution with different Δt .

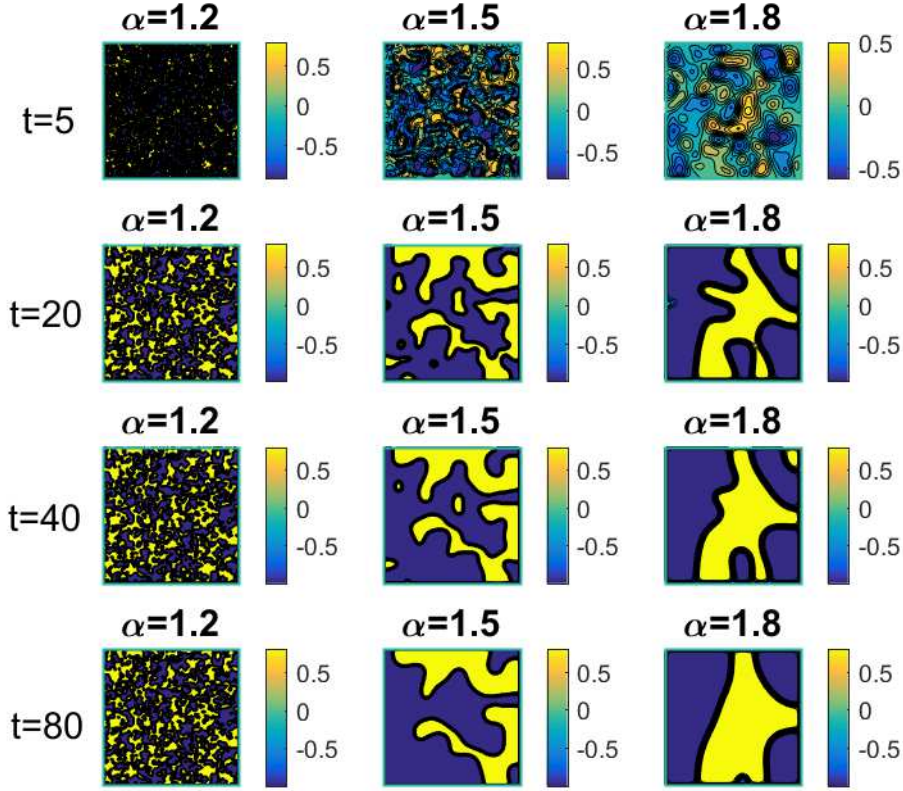


FIG. 5.5. Numerical dynamics (contour plots) with different fractional derivatives: $\alpha = 1.2, 1.5, 1.8$, where $h = 0.01, \varepsilon = 0.02, \Delta t = 0.5$.

heterogeneous phase structure. Moreover, it becomes slower for the phase coarsen process when the fractional order becomes smaller.

EXAMPLE 5.5. In this example, we consider the 3D space fractional Allen-Cahn equation with exact solution

$$(5.5) \quad u_0(x, y, z) = 0.1 \times \text{rand}(x, y, z) - 0.05,$$

where zero boundary values are set for the initial condition $u_0(x, y, z)$.

Again in this example, we first fix $h = 0.01, \alpha = 1.7, \varepsilon = 0.02$ but vary Δt .

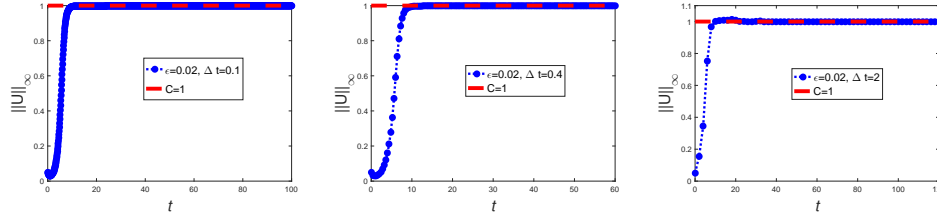


FIG. 5.6. Numerical results with $\alpha = 1.7, \varepsilon = 0.02$ and $h = 0.01$: the maximum values of solution with different Δt .

The maximum principle condition (4.4) also gives $0.1776 \leq \Delta t \leq 0.4945$ since the condition (4.4) does not rely on the dimension of the problem. Same as the 2D case, Figure 5.6 shows the maximum values of the numerical solutions are bounded by 1 when $\Delta t = 0.1$ and $\Delta t = 0.4$. However, discrete maximum principle is invalid when Δt increases to 2.

Finally, we also investigate the effects of fractional diffusion on phase separation and coarsening process. We set $h = 0.01, \varepsilon = 0.02, \Delta t = 0.5$ and $\alpha = 1.2, 1.5, 1.8$. Starting from random initial values, the snapshots of the contours for the numerical solutions at $t = 5, 20, 40, 80$ on the plane $z = 0.5$ are shown in Figure 5.7. Again, we see that reducing the fractional order yields to a thinner interfaces and it becomes slower for the phase coarsen process when the fractional order becomes smaller.

6. Conclusions. In this paper, we developed a fourth-order maximum principle preserving operator splitting scheme for the space fractional Allen-Cahn equation. The second-order splitting method for the fractional Allen-Cahn equation splits the numerical procedure into three steps. The first and third steps involves an ordinary differential equation that can be solved analytically. The intermediate step involves a linear multidimensional space fractional diffusion equation, which is solved by the ADI method and fourth-order finite difference method. A simple analysis for first and third steps together with a Fourier analysis for second ADI step show that the proposed operator splitting method is unconditionally stable for smooth solutions. Additionally, under certain reasonable time step constraint, the discrete maximum principle is obtained. Finally, Richardson extrapolation is exploited to increase the temporal accuracy to fourth order. Numerical tests for both 2D and 3D space fractional Allen-Cahn equations are carried out, for fabricated smooth solutions, results show that the method is unconditionally stable and fourth-order accurate in both time and space variables. More importantly, the discrete maximum principle are numerically well verified.

The proposed linear scheme in this paper is fourth-order accurate, maximum principle preserving and unconditionally stable. However, discrete energy decay law is generally not satisfied. It will be very interesting to develop high-order linearized schemes with both discrete maximum principle and energy decreasing property. This will be our future objective.

REFERENCES

- [1] S.M. Allen, J.W. Cahn, A microscopic theory for antiphase boundary motion and its application to antiphase domain coarsening, *Acta Metall.*, 27 (1979), pp. 1085-1095.

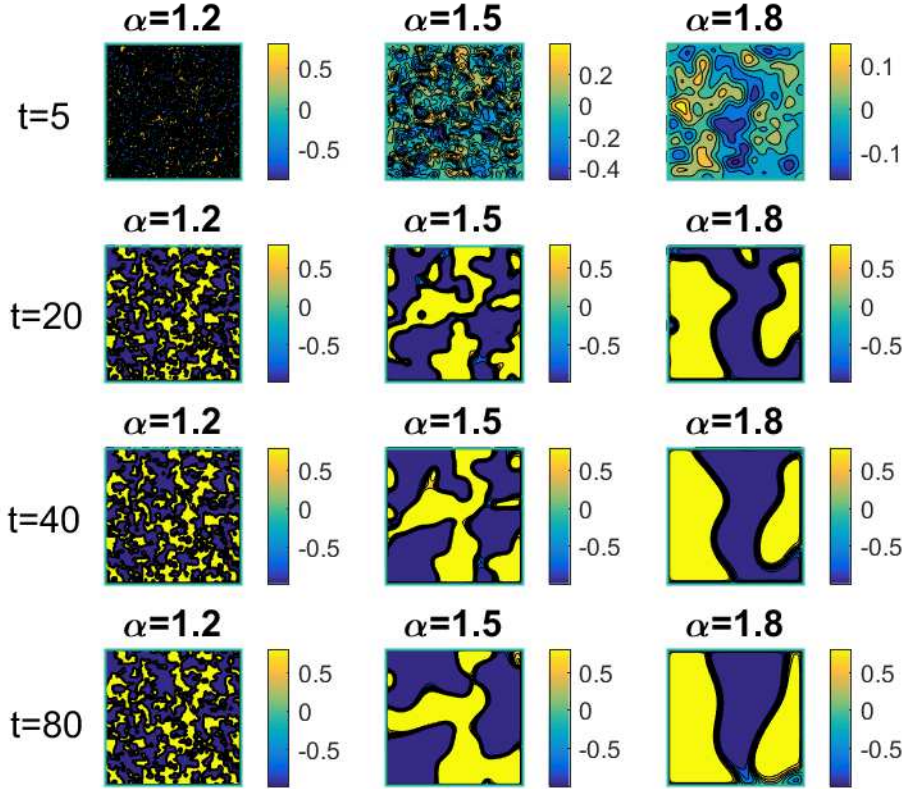


FIG. 5.7. Numerical dynamics (contour plots on the plane $z = 0.5$) with different fractional derivatives: $\alpha = 1.2, 1.5, 1.8$, where $h = 0.01, \varepsilon = 0.02, \Delta t = 0.5$.

- [2] A. Bueno-Orovio, D. Kay, K. Burrage, Fourier spectral methods for fractional-in-space reaction-diffusion equations, *BIT Numer. Math.*, 54 (2014), pp. 937-954.
- [3] K. Burrage, N. Hale, D. Kay, An efficient implicit FEM scheme for fractional-in-space reaction-diffusion equations, *SIAM J. Sci. Comput.*, 34 (2012), pp. A2145-A2172.
- [4] H. Chan, J. Wei, Traveling wave solutions for bistable fractional Allen-Cahn equations with a pyramidal front, *J. Differ. Equations*, 262 (2017), pp. 4567-4609.
- [5] C. Çelik, M. Duman, Crank-Nicolson method for the fractional diffusion equation with the Riesz fractional derivative, *J. Comput. Phys.*, 231 (2012), pp. 1743-1750.
- [6] B. Chen, D. He, K. Pan, A linearized high-order combined compact difference scheme for multi-dimensional coupled Burgers equations, *Numer. Math.-Theory Me.*, 11(2) (2018), pp. 299-320.
- [7] J.W. Choi, H.G. Lee, et al., An unconditionally gradient stable numerical method for solving the Allen-Cahn equation, *Physica A*, 388 (2009), pp. 1791-1803.
- [8] M. Dehghan, M. Abbaszadeh, W. Deng, Fourth-order numerical method for the space-time tempered fractional diffusion-wave equation, *Appl. Math. Lett.*, 73 (2017), pp. 120-127.
- [9] Q. Du, C. Liu, X. Wang, A phase field approach in the numerical study of the elastic bending energy for vesicle membranes, *J. Comput. Phys.*, 198 (2004), pp. 450-468.
- [10] L.C. Evans and J. Spruck, Motion of level sets by mean curvature, I, *J. Diff. Geom.*, 33 (1991), pp. 635-681.
- [11] L.C. Evans, H. M. Sonner and P.E. Souganidis, Phase transitions and generalized motion by mean curvature, *Comm. Pure Appl. Math.*, 45 (1992), pp. 1097-1123.
- [12] X. Feng, A. Prohl, Numerical analysis of the Allen-Cahn equation and approximation for mean curvature flows, *Numer. Math.*, 94 (2003), pp. 33-65.
- [13] X. Feng, T. Tang and J. Yang, Stabilized Crank-Nicolson/Adams-Bashforth schemes for phase

- field models, *E. Asian. J. Appl. Math.*, 3 (2013), pp. 59-80.
- [14] X. Feng, H. Song, et al., Nonlinearly stable implicit-explicit methods for the Allen-Cahn equation, *Inverse Probl. Imag.*, 7 (2013), pp. 679-695.
 - [15] C. Gui, M. Zhao, Traveling wave solutions of Allen-Cahn equation with a fractional Laplacian, *Ann. I. H. Poincaré-An.*, 32(4) (2015), pp. 785-812.
 - [16] Z. Hao, Z. Sun, A linearized high-order difference scheme for the fractional Ginzburg-Landau equation, *Numer. Meth. Part. D. E.*, 33 (2017), pp. 105-124.
 - [17] D. He, K. Pan, An unconditionally stable linearized difference scheme for the fractional Ginzburg-Landau equation, *Numer. Algorithms*, (2018), <https://link.springer.com/article/10.1007/s11075-017-0466-y>.
 - [18] D. He and K. Pan, An unconditionally stable linearized CCD-ADI method for generalized nonlinear Schrödinger equations with variable coefficients in two and three dimensions, *Comput. Math. Appl.*, 73 (2017), pp. 2360-2374.
 - [19] D. He, K. Pan, A Fifth-Order Combined Difference Scheme for Stokes Flow on Polar Geometries, *E. Asian J. Appl. Math.*, 7(4) (2018), pp. 714-727.
 - [20] T. Hou, T. Tang, J. Yang, Numerical Analysis of Fully Discretized Crank-Nicolson Scheme for Fractional-in-Space Allen-Cahn Equations, *J. Sci. Comput.*, 72 (2017), pp. 1214-1231.
 - [21] M. Ilić, F. Liu, et al., Numerical approximation of a fractional-in-space diffusion equation, *Fract. Calc. Appl. Anal.*, 8 (2005), pp. 323-341.
 - [22] X. Lin, N. Ng, H. Sun, A multigrid method for linear systems arising from time-dependent two-dimensional space-fractional diffusion equations, *J. Comput. Phys.*, 336 (2017), pp. 69-86.
 - [23] C. Liu, J. Shen, A phase field model for the mixture of two incompressible fluids and its approximation by a Fourier-spectral method, *Physica D.*, 179 (2003), pp. 211-228.
 - [24] H.G. Lee, J.Y. Lee, A semi-analytical Fourier spectral method for the Allen-Cahn equation. *Comput. Math. Appl.*, 68 (2014), pp. 174-184.
 - [25] H.G. Lee, J.Y. Lee, A second order operator splitting method for Allen-Cahn type equations with nonlinear source terms, *Phys. A*, 432 (2015), pp. 24-34.
 - [26] T.A.M. Langlands, B.I. Henry, The accuracy and stability of an implicit solution method for the fractional diffusion equation, *J. Comput. Phys.*, 205 (2005), pp. 719-736.
 - [27] X.J. Li, C.J. Xu, A space-time spectral method for the time fractional diffusion equation, *SIAM J. Numer. Anal.*, 47 (2009), pp. 2108-2131.
 - [28] Y.M. Lin, C.J. Xu, Finite difference/spectral approximations for the time-fractional diffusion equation, *J. Comput. Phys.*, 225 (2007), pp. 1533-1552.
 - [29] Y. Nec, A.A. Nepomnyashchy, A.A. Golovin, Front-type solutions of fractional Allen-Cahn equation, *Physica D*, 237 (2008), pp. 3237-3251.
 - [30] H. Moghaderi, M. Dehghan, M. Donatelli, M. Mazza, Spectral analysis and multigrid preconditioners for two-dimensional space-fractional diffusion equations, *J. Comput. Phys.*, 350 (2017), pp. 992-1011.
 - [31] J. Pan, R. Ke, et al., Preconditioning techniques for diagonal-times-Toeplitz matrices in fractional diffusion equations, *SIAM J. Sci. Comput.*, 36 (2014), pp. A2698-A2719.
 - [32] H. Pang, H. Sun, Multigrid method for fractional diffusion equations, *J. Comput. Phys.*, 231 (2012), pp. 693C703.
 - [33] D. Peaceman and H. Rachford, The numerical solution of parabolic and elliptic differential equations, *J. Soc. Ind. Appl. Math.*, 3 (1955), pp. 28-41.
 - [34] A. Saadatmandi, M. Dehghan, A tau approach for solution of the space fractional diffusion equation, *Comput. Math. Appl.*, 62 (2011), pp. 1135-1142.
 - [35] J. Shen, T. Tang, J. Yang, On the maximum principle preserving schemes for the generalized Allen-Cahn equation. *Commun. Math. Sci.*, 14 (2016), pp. 1517-1534.
 - [36] J. Shen and X. Yang, Numerical approximations of Allen-Cahn and Cahn-Hilliard equations, *Discret. Contin. Dyn. Syst.*, 28 (2010), pp. 1669-1691.
 - [37] F. Song, C. Xu, G. Karniadakis, A fractional phase-field model for two-phase flows with tunable sharpness: Algorithms and simulations, *Comput. Methods Appl. Mech. Engrg.*, 305 (2016), pp. 376-404.
 - [38] G. Strang, On the construction and comparison of difference schemes, *SIAM J. Numer. Anal.*, 5 (1968), pp. 506-517.
 - [39] H. Sun and L. Li, A CCD-ADI method for unsteady convection-diffusion equations, *Comput. Phys. Commun.*, 185 (2014), pp. 790-797.
 - [40] T. Tang, J. Yang, Implicit-explicit scheme for the Allen-Cahn equation preserve the maximum principle, *J. Comput. Math.*, 34 (2016), pp. 451-461.
 - [41] W. Tian, H. Zhou, W. Deng, A class of second order difference approximation for solving space fractional diffusion equations, *Math. Comput.*, 84 (2015), pp. 1703-1727.

- [42] P. Wang, C. Huang, An implicit midpoint difference scheme for the fractional Ginzburg-Landau equation, *J. Comput. Phys.*, 312 (2016), pp. 31-49.
- [43] P. Wang, C. Huang, L. Zhao, Point-wise error estimate of a conservative difference scheme for the fractional Schrödinger equation, *J. Comput. Appl. Math.*, 306 (2016), pp. 231-247.
- [44] X. Yang, Error analysis of stabilized semi-implicit method of Allen-Cahn equation, *Discrete Contin. Dyn. B*, 11 (2009), pp. 1057-1070.
- [45] X. Yang, J. Feng, et al., Numerical simulations of jet pinching-off and drop formation using an energetic variational phase-field method, *J. Comput. Phys.*, 218 (2006), pp. 417-428.
- [46] Q. Yang, F. Liu, I. Turner, Numerical methods for fractional partial differential equations with Riesz space fractional derivatives, *Appl. Math. Model.*, 34 (2010), pp. 200-218.
- [47] P. Yue, J. Feng, et al., Diffuse-interface simulations of drop coalescence and retraction in viscoelastic fluids, *J. Non-Newtonian Fluid Mech.*, 129 (2005), pp. 163-176.
- [48] P. Yue, C. Zhou, et al., Phase-field simulations of interfacial dynamics in viscoelastic fluids using finite elements with adaptive meshing, *J. Comput. Phys.*, 219 (2006), pp. 47-67.
- [49] S.B. Yuste, L. Acedo, An explicit finite difference method and a new Von Neumann-type stability analysis for fractional diffusion equations, *SIAM J. Numer. Anal.*, 42 (2005), pp. 1862-1874.
- [50] S. Zhai, X. Feng, Y. He, Numerical simulation of the three dimensional Allen-Cahn equation by the high-order compact ADI method, *Comput. Phys. Commun.*, 185 (2014), pp. 449-2455.
- [51] S. Zhai, Z. Weng, X. Feng, Fast explicit operator splitting method and time-step adaptivity for fractional non-local Allen-Cahn model, *Appl. Math. Model.*, 40 (2016), pp. 1315-1324.
- [52] L. Zhang, H. Sun, H. Pang, Fast numerical solution for fractional diffusion equations by exponential quadrature rule, *J. Comput. Phys.*, 299 (2015), pp. 130-143.
- [53] J. Zhang, Q. Du, Numerical studies of discrete approximations to the Allen-Cahn equation in the sharp interface limit, *SIAM J. Sci. Comput.*, 31 (2009), pp. 3042-3063.
- [54] P. Zhuang, F. Liu, V. Anh, I. Turner, Numerical methods for the variable-order fractional advection diffusion equation with a nonlinear source term, *SIAM J. Numer. Anal.*, 47 (2009), pp. 1760-1781.